Optical O-band soliton comb generation in photonic integrated silicon nitride microresonator chips

Xingxing Ding
Key Laboratory of Specialty Fiber Optics and Optical Access Networks Shanghai University, Shanghai 200444, China

Suwan Sun
Key Laboratory of Specialty Fiber Optics and Optical Access Networks Shanghai University, Shanghai 200444, China

Zhiming Shi
Key Laboratory of Specialty Fiber Optics and Optical Access Networks Shanghai University, Shanghai 200444, China

Baoqi Shi
International Quantum Academy, Shenzhen 518048, China

Chen Shen
International Quantum Academy, Shenzhen 518048, China

Haiyan Jia
Qaleido Photonics, Hangzhou 310000, China

Zhichao Ye
Qaleido Photonics, Hangzhou 310000, China

Junqiu Liu
International Quantum Academy, Shenzhen 518048, China

Hairun Guo*
Key Laboratory of Specialty Fiber Optics and Optical Access Networks Shanghai University, Shanghai 200444, China
hairun.guo@shu.edu.cn

***Abstract*—We implement both coherent and decoherent optical microcombs in the O-band, in chip-scale Si_3N_4 microresonators featuring both high-quality factors and moderate anomalous dispersion, which are readily for applications from time-resolved spectroscopy, telecommunications, to coherent tomography.**

Keywords—optical O-band, soliton comb, silicon nitride waveguides

I. Introduction

Soliton microcombs in miniatured and chip scale optical microresonators have unprecedentedly extended the performance of optical frequency combs, by forming temporal dissipative solitons in the ultrafast and ultrabroadband form[1]. In principle, governed by the dispersion as well as the nonlinearity of the cavity, these solitons could have a repetition frequency in the microwave range (10~1000 GHz), with wavelength spanning a few hundred of nanometers. The intrinsic phase alignment of solitons is beneficial for a number of applications, including coherent telecommunications[2], massive parallel LiDAR[3], low noise photonic microwave synthesis[4] [5], astronomical calibration[6], among others. To date, most soliton microcombs were demonstrated in the optical C-band (i.e. at around 1550 nm), yet are prone to distortion given the dispersion in optical fibers that are often used to guide the light wave.

Apart from the C-band, optical O-band is equally of interest. This wavelength range is recognized as both the low-dispersion window for optical fiber communications, and the window for biochemical imaging. Efforts have been reported to generate both dissipative soliton-based frequency combs[7], or chaotic combs[8] in the O-band, aiming at optical metrology or biomedical coherent tomography, respectively. To access such combs, anomalous dispersion is usually required, which in most cases are supported in chip integrated platforms (e.g. silicon nitride) with the state of the art photonic micro- and nano- fabrication. Indeed, with lithographically controlled dispersion engineering, anomalous dispersion over a wide wavelength range is supported in silicon nitride waveguide based microresonators with a film thickness typically beyond 800 nm[9]. This has opened the access for O-band microcombs both in the coherent and decoherent regime. Yet, pure dissipative solitons governed by the anomalous group velocity dispersion (GVD) have not been accessed in the O-band, with potential challenges in maintaining both high quality factors and sufficiently strong dispersion in this range. Alternatively, in a silica rod microresonator platform, a stabilized soliton wave-form in the close-to-zero dispersion regime was demonstrated[10].

Here, we demonstrate both coherent and decoherent optical microcombs in the O-band, in photonic chip integrated Si_3N_4 microresonator chips, which feature both high quality factors (Q_0>10^7) and moderate anomalous GVD, from a foundry manufacturing process on 6-inch wafers. In particular, pure dissipative solitons with a repetition frequency of ca. 200GHz were implemented.

II. Characterization of Microresonators

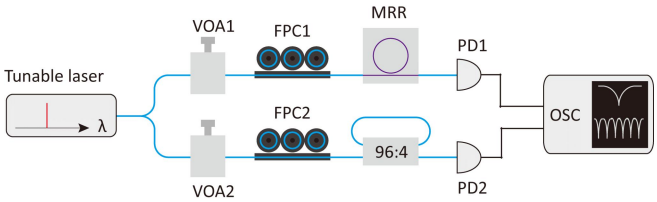

Fig.1 Experimental setup for dispersion and linewidth measurement regarding the Si_3N_4 microresonator, where the frequency calibration is via a fiber-loop cavity (FSR~41.4MHz). VOA: variable optical attenuator, FPC: fiber polarization control, PD: photodetector, OSC: oscilloscope.

In experiments, photonic integrated Si_3N_4 microresonator chips are fabricated at the foundry *Qaleido Photonics*, in which each resonator consists of a ring waveguide as the cavity and a bus waveguide for evanescent wave coupling to the cavity. The waveguide core is Si_3N_4, and the cladding is SiO_2. In the selected microresonator, the ring has a radius of 114 μm and has a cross section of 1800 × 780 nm^2. This microresonator is first characterized by measuring the dispersion as well as the resonance linewidth. In this measurement, the frequency calibration is carried out by using an optical fiber loop cavity. The experimental setup is shown in Fig.1, in which a tunable laser (SANTEC TSL-550)

XXX-X-XXXX-XXXX-X/XX/$XX.00 ©20XX IEEE

is coupled to the microresonator chip by a pair of lensed fiber. The coupling efficiency is ~47% per facet.

When the laser frequency is continuously swept, it features a number of cavity resonances. A fraction of the laser is simultaneously coupled to the fiber-loop cavity with a free spectral range (FSR) of 41.4 MHz (measured with an electro-optical modulator). The transmission traces of the two cavities are displayed on the oscilloscope at the same time. Both power traces can be calibrated and mapped to the frequency axis, and fiber-loop cavity can be used as the reference cavity to represent the information such as the resonant frequency and the linewidth of the optical microresonator. In mathematics, the resonant frequency ω_μ can be expressed in a Taylor series, and integrated dispersion as

$$D_{int}(\mu) = \omega_\mu - \omega_0 - D_1\mu = \sum_{m\geq 2} \frac{D_m \mu^m}{m!}$$

where ω_0 indicates the frequency of a central resonant mode ($\mu = 0$), D_m indicates the m-th order component of ω_μ with respect to the central mode. $D_1/2\pi$ corresponds to the FSR of the microresonator, and $D_2/2\pi$ indicates the GVD of the cavity.

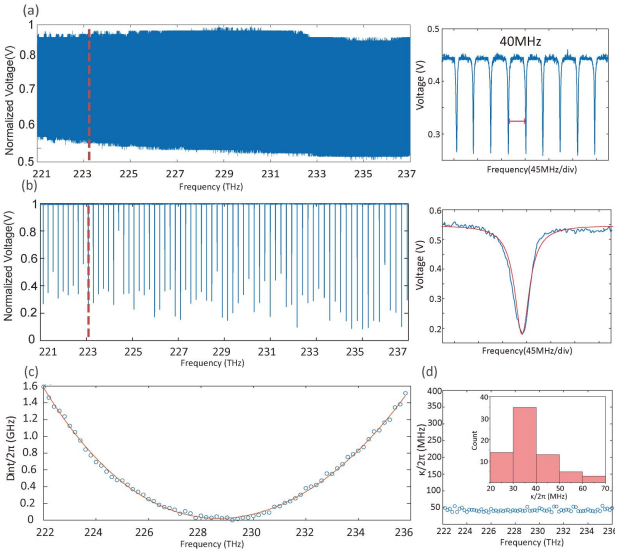

Fig.2 (a,b) Transmission trace of both the microresonator and the fiber-loop cavity and local magnification. (c) Extracted integrated dispersion. (d) The distribution of the resonance linewidths. The inset is a histogram of the linewidth, which indicates that the statistic linewidth of the microresonator is ca. 40MHz.

Since the fiber dispersion is low in the O-band, frequency calibration using the fiber-loop cavity could have decent accuracy compared with that in the C-band. As a result, in the range from 221-237 THz, more than seventy resonant frequencies of the TE_{00} mode are recorded (Fig. 2b). Each resonance is Lorentzian-fitted to extract the resonant frequency as well as the linewidth. Afterwards, the integral dispersion distribution is retrieved (Fig. 2c). The estimated FSR of the cavity is 199 GHz and the GVD is $D_2/2\pi = 2.1$ MHz at the optical frequency of 229 THz. In addition, the statistic distribution of the resonance linewidth is analyzed, showing a primary linewidth of ~40 MHz (Fig. 2d), which corresponds to a loaded Q factor of 5.7×10^6.

III. Optical Comb Generation

We next carried out experiments on the soliton microcomb generation in the above mentioned Si_3N_4 microresonator chip, via the laser tuning scheme. As shown in Fig.3a, a narrow-linewidth tunable laser (Toptica CTL1310) is tuned by an arbitrary function generator and power amplified by a Raman laser amplifier before coupled into the microresonator. The transmitted light after the microresonator is characterized both in the optical spectrum and in the low-frequency RF spectrum.

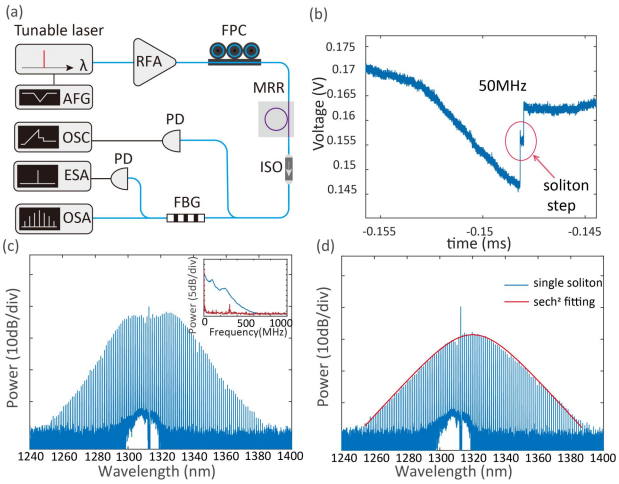

Fig.3 Soliton microcomb generation in a Si_3N_4 microresonator. (a) Schematic of the experimental setup. AFG: arbitrary function generator, RFA: Raman Fiber Amplifier, OSC: oscilloscope, ESA: electrical spectrum analyzer, and OSA: optical spectrum analyzer. (b) The generated power trace. The trace shows a triangle profile with a stair-like pattern at the ending edge (also called the soliton step), implying that the soliton microcomb can be accessed. (c,d) Measured comb spectra in the MI state and single-soliton state. Inset: After the residual pumping wave in the combs is filtered out, low-frequency RF spectra of both the soliton state(red) and a comb in the MI state(blue), respectively.

When the pump power is scanned over a cavity resonance (wavelength ~1312.28 nm), from the blue to the red detuned side, and in the power of ca. 400 mW, a typical triangular trace in the transmission is observed, which also features a step-like pattern (Fig. 3b) indicating the existence of dissipative solitons in the resonator. In the experiment, the observed soliton step was as long as ~50 MHz. When the laser frequency is stopped at the soliton step, soliton comb is accessed. In particular, the single-soliton state with a clear hyperbolic secant ($sech^2$) spectral profile can be implemented (Fig. 3d), which is recognized as a pure dissipative soliton mostly governed by the anomalous GVD. In contrast, if the laser frequency is controlled at the bottom of the transmission trace, a chaotic comb in the regime of modulation instability is observed (Fig. 3c). Both the soliton comb and the chaotic comb are characterized in the low-frequency RF domain, which has the residual pump wave filtered out before the photodetection. While the chaotic comb shows a broadband noisy RF spectrum, the soliton comb is much stabilized, yet with a weak frequency tone at ca. 350 MHz. This implies that the soliton is not purely stabilized but shows certain breathing dynamic[11]. In addition, the overall power of the chaotic comb is higher than that of the soliton comb. Still, the power of the soliton comb can be further amplified using e.g. active doped gain fibers or by means of nonlinear parametric processes. In this regard, the soliton in the low-dispersion window of optical fibers could have its profile well preserved over the propagation of

meters distance, and an effective soliton waveform amplification is also expectable.

IV. Conclusions

In conclusion, we have characterized the microresonator in O-band, and achieved pure quadratic solitons at 1310 nm pump on the chip integrated Si_3N_4 microresonator due to the anomalous GVD and decent Q-factor. The soliton micrcombs in O-band has enabled the signal maintance over long distance, which will promote the development of long-distance coherent communication. The decoherent microcombs in O band has also a great potential in biomedical coherent tomography.

Acknowledgment

This work was funded by the National Key Research and Development Program of China (2020YFA0309400), the National Natural Science Foundation of China (11974234), and the Shanghai Science and Technology Development Foundation (20QA1403500).

References

[1] T. J. Kippenberg, A. L. Gaeta, M. Lipson, and M. L. Gorodetsky, “Dissipative Kerr solitons in optical microresonators,” Science, vol. 361, no. 6402, p. eaan8083, 2018.

[2] P. Marin-Palomo et al., “Microresonator-based solitons for massively parallel coherent optical communications,” Nature, vol. 546, no. 7657, pp. 274–279, Jun. 2017.

[3] J. Riemensberger et al., “Massively parallel coherent laser ranging using a soliton microcomb,” Nature, vol. 581, no. 7807, pp. 164–170, May 2020.

[4] W. Liang et al., “High spectral purity Kerr frequency comb radio frequency photonic oscillator,” Nature Communications, vol. 6, no. 1, p. 7957, Aug. 2015.

[5] J. Liu et al., “Photonic microwave generation in the X- and K-band using integrated soliton microcombs,” Nature Photonics, vol. 14, no. 8, pp. 486–491, Aug. 2020.

[6] E. Obrzud et al., “A microphotonic astrocomb,” Nature Photonics, vol. 13, no. 1, pp. 31–35, Jan. 2019.

[7] M. H. P. Pfeiffer et al., “Octave-spanning dissipative Kerr soliton frequency combs in Si_3N_4 microresonators,” Optica, vol. 4, no. 7, pp. 684–691, 2017.

[8] X. Ji et al., “Chip-based frequency comb sources for optical coherence tomography,” Opt. Express, vol. 27, no. 14, pp. 19896–19905, 2019.

[9] Z. Ye et al., “Foundry manufacturing of tight-confinement, dispersion-engineered, ultralow-loss silicon nitride photonic integrated circuits,” Photon. Res., PRJ, vol. 11, no. 4, pp. 558–568, Apr. 2023.

[10] S. Zhang, T. Bi, and P. Del’Haye, “Microresonator Soliton Frequency Combs in the Zero-Dispersion Regime.” arXiv, Sep. 15, 2022.

[11] E. Lucas, M. Karpov, H. Guo, M. L. Gorodetsky, and T. J. Kippenberg, “Breathing dissipative solitons in optical microresonators,” Nature Communications, vol. 8, no. 1, p. 736, Sep. 2017.